Applied Catalysis B: Environmental 92 (2009) 68–74

Contents lists available at ScienceDirect

Applied Catalysis B: Environmental

journal homepage: www.elsevier.com/locate/apcatb

Hydrogen generation by hydrolysis of alkaline $NaBH_4$ solution with Cr-promoted Co–B amorphous catalyst

R. Fernandes *, N. Patel, A. Miotello

Dipartimento di Fisica, Università degli Studi di Trento, I-38100 Povo, Trento, Italy

ARTICLE INFO

Article history:
Received 5 June 2009
Received in revised form 14 July 2009
Accepted 20 July 2009
Available online 25 July 2009

Keywords:
H_2 generation
Hydrolysis
Sodium Borohydride
Co–Cr–B catalyst
Surface area

ABSTRACT

Cr-modified Co–B (Co–Cr–B) catalyst alloy powders have been synthesized by chemical reduction of cobalt and chromium salt at room temperature to study the hydrogen production by catalytic hydrolysis of $NaBH_4$. The Cr/Co molar ratio was varied in the catalyst in order to study the effect of Cr doping on surface modification and catalytic efficiency of Co–B catalyst. The resulting catalyst powders were characterized by scanning electron microscopy, X-ray diffraction, X-photoelectron spectroscopy, and BET surface area measurement. When the molar ratio χ_{Cr} = Cr/(Cr + Co) exceeds 9% the BET surface area of the Co–Cr–B catalyst increases by one order of magnitude as compared to that of Co–B catalyst. The catalytic activity of the Co–Cr–B for hydrogen production depends on Cr concentration: specifically, the activity increases by increasing χ_{Cr} up to about 4% and then it gradually decreases by further increasing χ_{Cr}. We established that the increased catalytic activity is related to the formation of chromium oxide on the catalyst surface, with the oxide favoring the dispersion of Co–B particles resulting in high catalyst surface area. However as χ_{Cr} exceeds 4%, Cr starts to cover the Co active sites and the corresponding catalytic activity decreases. The highest catalytic activity was obtained at the optimum Cr-content, χ_{Cr} = 4%, in Co–Cr–B catalyst, showing nearly 4 times higher H_2 generation rate than that of pure Co–B catalyst. Kinetic studies on the hydrolysis reaction of $NaBH_4$ with Co–Cr–B catalyst reveal that the concentrations of both $NaBH_4$ and NaOH have essentially no effects on hydrogen generation rate. The promoting effect of Cr in Co–Cr–B catalyst results in lower activation energy for hydrogen production, which is 37 kJ mol^{-1} as compared to 45 kJ mol^{-1} obtained with pure Co–B powder. Finally, the possible role of Cr^{3+} species in the electron exchange mechanisms involved in $NaBH_4$ hydrolysis with the Co–Cr–B catalyst has been discussed.

1. Introduction

Research on clean renewable energy is important to try solving problems related to emission of greenhouse gases from fossil fuels, which contribute to dangerous climatic changes. Hydrogen, with its high gravimetric energy density, is a promising route to store renewable energy. Moreover, there is almost zero emission of environment pollutants when hydrogen is used as a fuel in proton exchange membrane fuel cell (PEMFC) [1]. However, for a real clean hydrogen-based technology it is essential to develop safe and convenient hydrogen storage and production systems.

Considerable efforts have been focused on hydrogen storage in pressurized tanks of gas or liquid, in metal alloys, and on activated- or nanotubes-carbon [2]. Unfortunately, all these systems lack gravimetric and/or volumetric energy efficiency to meet the requirement for commercial application [3]. On-board hydrogen production is also becoming increasingly important as a potential route to supply hydrogen to PEMFC. Chemical hydrides ($NaBH_4$, $LiBH_4$, NaH, KBH_4, etc.) with high hydrogen storage gravimetric and volumetric efficiencies are the most potential candidates to supply pure hydrogen for portable application at room temperature [4,5].

Among the chemical hydrides, aqueous sodium borohydride ($NaBH_4$) seems to be an ideal hydrogen source because it is stable in alkaline solution, non-flammable, non-toxic in nature, and with hydrogen storage capability of 10.8 wt% [6]. The reaction product (borax), obtained after de-hydrogenation of $NaBH_4$, is environmentally clean and can be recycled to generate the reactant [7]. Hydrogen is generated by water-based hydrolysis reaction of $NaBH_4$, during which half of the produced hydrogen stems from the water solvent [8]. These distinct advantages of hydrogen generation from $NaBH_4$ hydrolysis make it a promising on-board hydrogen generation method for portable PEM fuel cells.

* Corresponding author.
E-mail address: fernandes@science.unitn.it (R. Fernandes).

0926-3373/$ – see front matter © 2009 Elsevier B.V. All rights reserved.
doi:10.1016/j.apcatb.2009.07.019

The hydrogen generation rate can be significantly enhanced by using catalyst during the hydrolysis reaction. Many organic and inorganic acids are able to enhance the hydrolysis reaction rate, but the reaction usually becomes uncontrollable [9]. On the other hand, solid state catalysts such as precious metals (generally functionalized with support) or transition metals and their salts are found to be very efficient in accelerating the hydrolysis reaction in a controllable manner. Noble catalysts like Pt [10] and Pd [11] supported on carbon, PtRu supported on metal oxide [12], Ru supported on anion-exchange resin [4], Ru nanoclusters [13], and Ru-promoted sulphated zirconia [14] have been utilized in the past to enhance the hydrogen production rate. However, these catalysts do not seem to be viable for industrial application considering their cost and availability. Transition metals such as fluorinated Mg based alloy [15], Raney Ni and Co, nickel and cobalt borides [16–18], and even metal salts are generally used to accelerate the hydrolysis reaction of $NaBH_4$. Cobalt boride (Co–B) is considered a good candidate owing to its relevant catalytic activity and low cost. Our previous reports prove that the alloy catalysts in the form of Co–Ni–B [19], Co–P–B [20], and Co–Ni–P–B [21] exhibit superior catalytic activity in hydrogen production by hydrolysis of $NaBH_4$.

Co–B catalyst material can be effortlessly synthesized by a simple chemical reduction method, in which transition metal ions are brought to the metallic state by a reducing agent [17]. However, the exothermic nature of this reaction causes Co–B particles to agglomerate due to the high surface energy involved. This agglomeration of particles lowers the effective surface area of the catalyst powder thus limiting the catalytic activity. In recent years, several routes have been indicated to increase the effective surface area of the Co–B catalyst. To limit agglomeration, Li et al. [22] adopted ultrasound-assisted reduction method to prepare uniform spherical Co–B amorphous alloy nanoparticles; here the particle size was adjusted by changing either the ultrasound power or the ultrasonication time. Another way to increase the catalyst surface area is by depositing Co–B on a support material having specific surface features like carbon [23], γ-Al_2O_3 [24], and Ni foam [25,26]. Tong et al. [27] and Ma et al. [28] synthesized mesoporous and hollow Co–B catalyst sphere, respectively, by using organic templates during the reduction reaction: the final surface area of these catalyst powders is much higher than that of the "normal" Co–B powder. Co–B catalysts synthesized in the form of nanoparticle assembled films by pulsed laser deposition technique, showed a performance similar to that of the noble metals because of the achieved high surface area [18,29]. An efficient route to avoid agglomeration of Co–B particles is by introducing atomic barrier using transition metals like Cr, Mo, or W [30]. These promoter metals, in the form of oxide, are so efficient that even a small atomic concentration is able to significantly increase the surface area of the metal-borides catalyst powder [31]. In addition, they also contribute to the overall catalytic reaction [31]. All these combined effects, along with the simple preparation method, make such catalysts very attractive.

In the present work, we have synthesized Cr-modified Co–B catalyst powders by chemical reduction method. The Co–Cr–B powders exhibit superior catalytic activity, as compared to pure Co–B powders, owing to their high surface area. The Cr/Co molar ratio was varied in the final catalyst in order to study the effect of chromium doping on the catalytic efficiency of the cobalt boride catalyst. The analysis, performed with several techniques, of the Co–Cr–B catalyst revealed that the surface chromium oxide acts as an atomic barrier to inhibit agglomeration of the Co–B nanoparticles thus increasing the active surface area. Finally, some suggestions are reported on the possible role of the Cr^{3+} species in the electron exchange mechanisms involved in the $NaBH_4$ hydrolysis with the Co–Cr–B catalyst.

2. Experimental

2.1. Catalyst preparation

Co–Cr–B powder catalyst was synthesized by chemical reduction method. Sodium borohydride ($NaBH_4$) was added, as a reducing agent, into an aqueous solution containing cobalt salt ($CoCl_2$) and chromium salt ($Cr(NO_3)_3$) under vigorous stirring. An excess amount of borohydride was used in order to completely reduce Co and Cr cations to metals. The black powder separated from the solution during the reaction course was filtered and then extensively washed with distilled water and ethanol before drying at around 323 K under continuous N_2 flow. The Cr/(Cr + Co) molar ratio (χ_{Cr}) was adjusted in the final Co–Cr–B catalyst powder by varying the molar concentration of $Cr(NO_3)_3$ in the aqueous solution. To make experimental comparison we also prepared Co–B powder with the same procedure as Co–Cr–B catalyst but in the absence of chromium salt.

2.2. Catalyst characterization

The surface morphology of all the catalyst powders was studied by scanning electron microscope (SEM-FEG, JSM 7001F, JEOL) equipped with energy-dispersive spectroscopy analysis (EDS, INCA PentaFET-x3) to determine the composition of the samples. Structural characterization of the catalyst powders was performed by conventional X-ray diffraction (XRD) using the Cu K_α radiation (λ = 1.5414 Å) in Bragg–Brentano (θ–2θ) configuration. Surface electronic states and the related atomic composition of the catalysts were established by using X-ray photoelectron spectroscopy (XPS). X-ray photoelectron spectra were acquired using a SCIENTA ESCA200 instrument equipped with a monochromatic Al K_α (1486.6 eV) X-ray source and a hemispherical analyzer. No electrical charge compensation was required to perform XPS analysis. The BET surface area of the powder catalysts was determined by nitrogen absorption at 77 K (Micromeritics ASAP 2010) after degassing.

2.3. Hydrogen generation measurement

For catalytic activity measurements, an alkaline-stabilized solution of sodium borohydride (pH 13, 0.025 ± 0.001 M) (Rohm and Haas) was prepared by addition of NaOH. The titre of reagent was independently measured through iodometric method [32]. The generated hydrogen quantity was measured through a gas volumetric method [33] that here we briefly describe. The reaction chamber is composed of a cylindrical flat flange vessel with off-centre bottom outlet valve and a stirrer guide at the bottom. It is surrounded by a jacket connected to a heating circulator bath for temperature control. The temperature is controlled within ±0.1 K by a water bath with a digital temperature controller. The reactor is closed by a flat flange lid with five necks 29/32 NS type. A pressure sensor is placed in one of the angular side sockets and a second sensor is placed outside the reactor to follow the ambient pressure. Hydrogen evolved from the reactor, equipped with a catalyst insertion device, can flow through the second angular side socket, which is connected to the measurement system through a polyurethane tube. An electronic precision balance accurately measures the weight of the water displaced by the hydrogen produced during the reaction course. From weight of displaced water and gas pressure, the amount of produced hydrogen is established. A detailed description of the measurement apparatus is reported in Ref. [33]. In all measurement runs, the catalyst was placed on the appropriate device inside the reaction chamber and the system was sealed. Catalyst powder was added to 200 ml of the above solution, at 298 K, under continuous stirring. To make comparison, the

stoichiometric cumulative hydrogen production yield (%) vs time was plotted instead of the hydrogen volume (ml) vs time.

2.4. Kinetic studies

Kinetic studies on $NaBH_4$ hydrolysis using Co–Cr–B catalysts were conducted by varying different process parameters such as solution temperature, starting concentration of NaOH and $NaBH_4$. Fresh Co–Cr–B catalyst was used for each kinetic data acquisition. H_2 generation rate was measured at different solution temperatures to determine the activation energy involved in the catalytic hydrolysis reaction. In addition, several solutions with varying concentrations of NaOH (0.25–2.50 M) and $NaBH_4$ (0.05–0.150 M) were prepared to investigate the corresponding activity of the solution, in which one parameter was varied while the other parameters were kept constant.

3. Results and discussion

3.1. Effect of Cr concentration

First of all, the effect of Cr concentration on catalytic activity was studied by varying the percentage of Cr/(Cr + Co) molar ratio (χ_{Cr}) from about 1% to 9% in the Co–Cr–B powder catalyst. Fig. 1 presents the hydrogen generation yield, as a function of time, measured by hydrolysis of alkaline $NaBH_4$ (0.025 M) solution using Co–Cr–B catalyst powder with different Cr concentrations. The inset of Fig. 1 shows the plot of maximum H_2 generation rate (R_{max}) as a function of χ_{Cr}. BET surface area, χ_{Cr} measured by EDS, and maximum H_2 generation rate are summarized in Table 1. The promoting effect of chromium on catalytic activity is so evident that also a small amount of doping (χ_{Cr} = ~1%) is able to double the activity of Co–B catalyst. The H_2 generation rate increases with Cr-content and reaches the maximum when χ_{Cr} is about 4%. With further increase of χ_{Cr}, the activity of the powder decreases (each measurement is repeated at least 3 times). From Table 1 it can be seen that the addition of Cr-promoter enhances the BET surface area. For the highest Cr doping, Co–Cr–B-9 (the notation Co–Cr–B-*n* stands for χ_{Cr} = *n*%, with *n* = 1, 2, ...), the surface area increases to a value of about 203 $m^2\ g^{-1}$, i.e., one order of magnitude higher than that of undoped Co–B catalyst powder.

In the following section we will see that the presence of Cr increases the active surface area of the Co–B catalysts by avoiding agglomeration of the Co–B particles. However, large Cr doping is harmful for the catalyst activity because Cr would cover most of the active Co sites. Thus a well-defined χ_{Cr} value is required (χ_{Cr} = 4%, as shown in Fig. 1) to attain the best conditions for the catalytic activity of Co–Cr–B catalyst. Catalysts with χ_{Cr} = 4% are investigated in the following sections.

Table 1
Percentage molar ratio of Cr/(Cr + Co), BET surface area, and catalytic activity of the as-prepared catalyst powders.

Catalyst powders	Percentage molar ratio of Cr/(Cr + Co) (χ_{Cr}) (%)	BET surface area ($m^2\ g^{-1}$)	Maximum H_2 generation rate (ml $min^{-1}\ g^{-1}$ catalyst)
Co–B	–	~19.90	~850
Co–Cr–B-1	1.05 ± 0.13	–	~1990
Co–Cr–B-2	2.34 ± 0.14	–	~2950
Co–Cr–B-3	3.06 ± 0.16	~37.35	~3250
Co–Cr–B-4	4.14 ± 0.17	~38.85	~3400
Co–Cr–B-5	5.74 ± 0.18	~46.15	~2860
Co–Cr–B-9	9.20 ± 0.20	~202.75	~2100

3.2. Catalyst activity measurement

Hydrogen generation yield was measured, as a function of time, during the hydrolysis of alkaline $NaBH_4$ (0.025 M) solution in the presence of Co–B and Co–Cr–B catalyst powders at 298 K (Fig. 2). χ_{Cr} of about 4% was used in Co–Cr–B catalyst. The expected total amount of H_2 was measured, irrespective of the type of catalyst used. The H_2 generation yield values reported in Fig. 2 were perfectly fitted by using a single exponential function as described by [20]:

$$[H_2](t) = [H_2]_{max} \times (1 - e^{-k_1 t}) = 4[[BH_4^-]_0 \times (1 - e^{-k_1 t})] \quad (1)$$

where $[BH_4^-]_0$ is the initial molar concentration of sodium borohydride in the solution and k_1 is the overall rate constant of the reaction. Eq. (1) and results of Fig. 2 indicate that hydrolysis reaction is first order reaction with respect to $NaBH_4$. In the present case the low hydride/catalyst ratio was used and thus, the first order kinetics involving diffusion of BH_4^- on the catalyst surface is the rate limiting step during the hydrolysis reaction (see discussion reported in Ref. [20]). In case of much higher values of the hydride/catalyst ratio a zero order kinetics is observed (this will be discussed later in Section 3.5). The Co–Cr–B catalyst shows much higher catalytic activity for hydrogen generation as compared to the same amount (15 mg) of Co–B powder. A numerical procedure, described elsewhere [29], was utilized to obtain the maximum

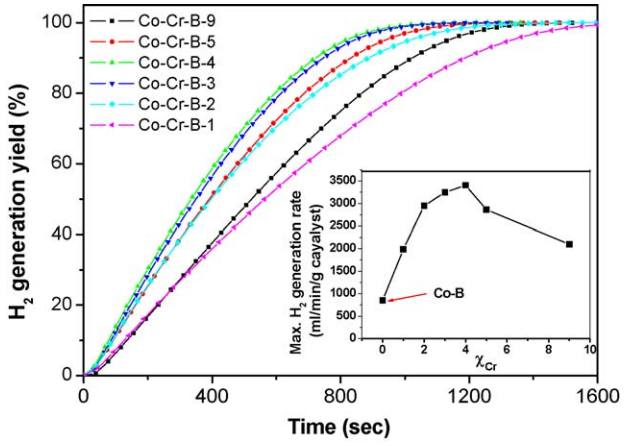

Fig. 1. Hydrogen generation yield as a function of reaction time obtained by hydrolysis of alkaline $NaBH_4$ (0.025 M) with Co–Cr–B catalyst with different Cr/(Cr + Co) molar ratios ranging from 1% to 10%. Inset shows the maximum H_2 generation rate (R_{max}) obtained with Co–Cr–B catalyst as a function of χ_{Cr}.

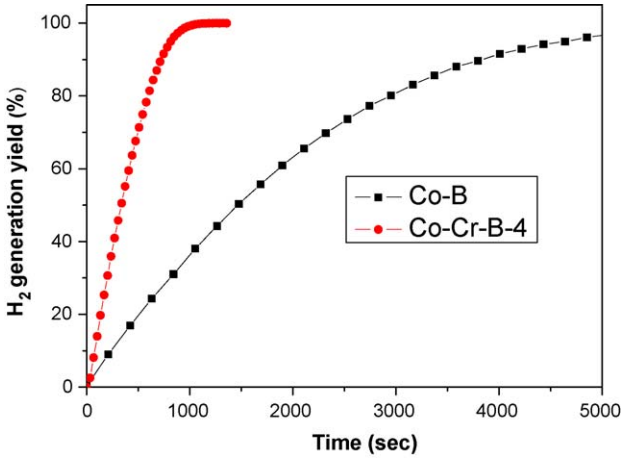

Fig. 2. Hydrogen generation yield as a function of reaction time obtained by hydrolysis of alkaline $NaBH_4$ (0.025 M) with Co–B and Co–Cr–B (χ_{Cr} = 4%) catalyst powders.

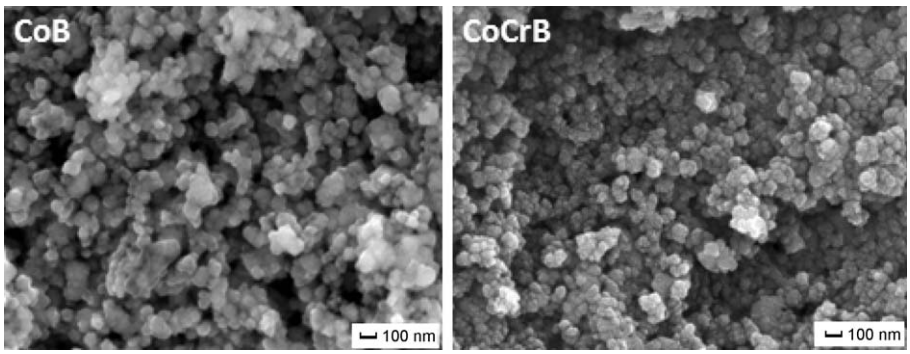

Fig. 3. SEM micrographs of Co–B and Co–Cr–B (χ_{Cr} = 4%) catalyst powders.

value of the hydrogen generation rate (R_{max}) for all the catalyst powders: these values are summarized in Table 1. The maximum H_2 generation rate obtained with χ_{Cr} = 4% catalyst is ~3400 ml min^{-1} g^{-1}, which is 4 times higher than that achieved with only Co–B catalyst powder (~850 ml min^{-1} g^{-1}). The above result clearly shows that addition of small amount of chromium in Co–B catalyst is able to significantly enhance the catalytic activity.

3.3. Catalyst characterization

In Fig. 3 we present SEM images of Co–B and Co–Cr–B (χ_{Cr} = 4%) powders. The SEM images of both catalyst powders show similar particle-like morphology with particles having spherical shape and size of a few nanometers. During the catalyst preparation, the use of $NaBH_4$ as a reducing agent causes a fast reduction of Co ions, which inhibit relevant particle growth. SEM image of Co–B catalyst shows agglomeration of the small particles. On the contrary, the catalyst doped with chromium consists of much more uniform particle size distribution with less amount of agglomeration and such a morphology is helpful to enhance the active surface area of catalysts. XRD patterns (Fig. 4) of Co–B, and Co–Cr–B (χ_{Cr} = 4%) powders show a broad peak at around $2\theta = 45^\circ$, which is attributed to the amorphous state of cobalt-metalloid alloy [34]. In addition, the broad peak at around $2\theta = 35^\circ$ attributed to the presence of Cr_2O_3 is observed for Co–Cr–B catalyst powder. Finally, the diffraction spectra indicate short-range order and long-range disorder and both features might contribute to enhance the catalytic activity [35]. Here we also report that all the Co–Cr–B catalyst powders, irrespective of the χ_{Cr} value, are almost amorphous and exhibit particle-like morphology with uniform dispersion of particles (figure not shown).

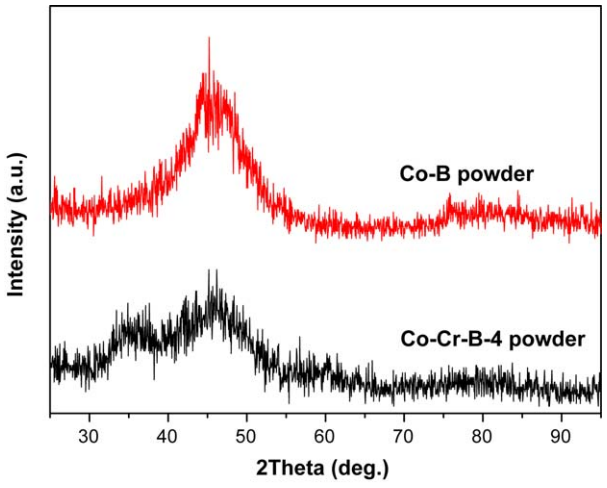

Fig. 4. XRD pattern of Co–B and Co–Cr–B (χ_{Cr} = 4%) catalyst powders.

XPS was used to gain insight into the electronic state and surface interaction between atoms in Co–B and Co–Cr–B compounds to understand the promoting effect of chromium to enhance the catalytic activity of Co–B. Fig. 5 shows the XPS spectra of $Co_{2p3/2}$, Cr_{2p}, and B_{1s} electronic levels in fresh Co–B and Co–Cr–B (χ_{Cr} = 4%) catalyst powders. For both catalyst powders, two peaks appear corresponding to the $Co_{2p3/2}$ level at the binding energies (BE) of 778.4 and 781.6 eV, indicating that Co element exists in both elemental and oxidized states, respectively. The 2+ state related to the peak of the oxidized cobalt is attributed to $Co(OH)_2$: this molecule would have been formed possibly during the catalyst preparation [36,37] or when it was exposed to ambient atmosphere before transfer to the reaction chamber. There is no shift in the present Co BE peak as compared to the standard binding energy of metallic Co. Two XPS peaks are also observed at BE values of 188.3 and 192.1 eV, which correspond to elemental and oxidized B_{1s} levels in Co–B and Co–Cr–B, respectively [36]. A positive shift of 1.2 eV is evident when comparing the BE of pure boron (187.1 eV) [38] to that of boron in the catalyst. This shift indicates electron transfer from alloying B to vacant d-orbital of metallic Co, which makes the boron atom electron deficient and the cobalt atom electron enriched: this is true for both catalyst powders [39]. These electron-enriched metal active sites repel the adsorption of oxygen atoms from the ambient atmosphere, while they are strongly adsorbed by the electron-deficient B. In other words, alloying B effectively protects metals from oxidation in ambient condition [40,41]. The lack of shift in Co peak of compound catalyst is due to the heavy mass of the atom. On the other hand, the Cr_{2p} spectrum for Co–Cr–B catalysts exhibits two peaks at 575.7 and 585.3 eV, attributed to $Cr_{2p3/2}$ and $Cr_{2p1/2}$ peaks of Cr^{3+} species, respectively [42], and thus we ascribe it to Cr_2O_3. This result is in agreement to XRD pattern, which describes that all the Cr particles are in oxidized state. It is also noticed that chromium does not modify the electronic interaction between Co and B because their relevant BEs remain unchanged after the Cr addition. Studies on oxidation processes of the elements, possibly occurring during and/or after hydrolysis reaction are planned for future research activity.

The BET surface area of Co–B and Co–Cr–B (χ_{Cr} = 4%) results to be 19.9 and 38.9 m^2 g^{-1}, respectively. Thus it shows that chromium doping of Co–B increases the specific surface area by almost 2 times, a result, which is due to the limited particle agglomeration process in Co–Cr–B as compared to Co–B (see Fig. 3).

Characterization results of Co–Cr–B catalyst powder suggest that chromium in the form of Cr_2O_3 is located on the surface of the catalyst. The chromium oxide acts as a kind of barrier between the several Co–B nanoparticles leading to smaller particle size with uniform distribution thus avoiding agglomeration because of their

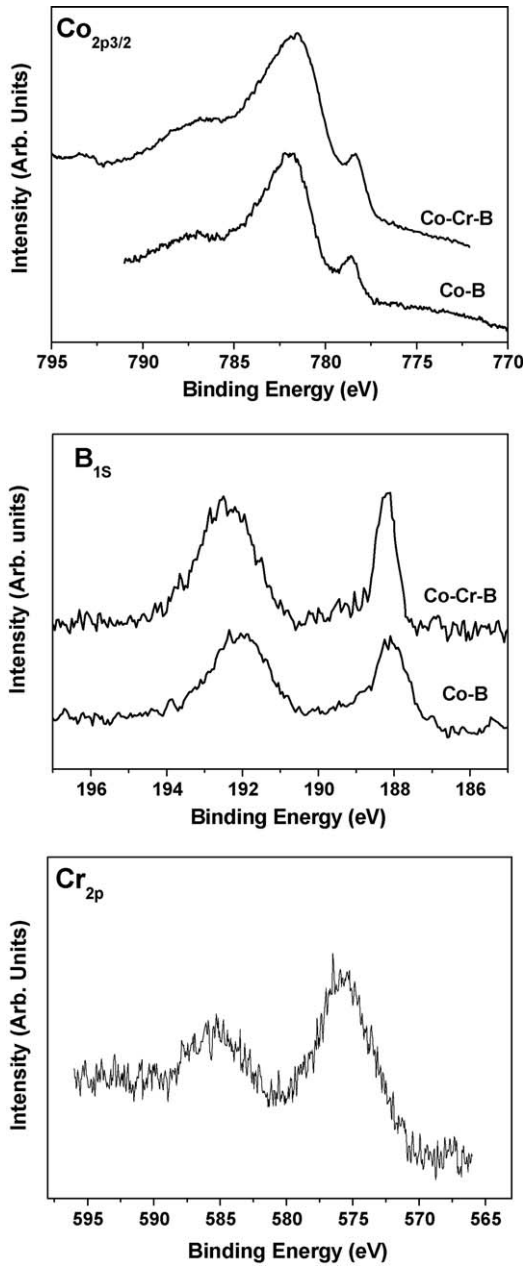

Fig. 5. X-ray photoelectron spectra of $Co_{2p3/2}$, Cr_{2p}, and B_{1s} levels for Co–B and Co–Cr–B (χ_{Cr} = 4%) catalyst powders.

high surface energy. As a result the effective surface area increases significantly in chromium-modified Co–B catalyst. Thus the enhanced catalytic activity for hydrogen generation by hydrolysis of $NaBH_4$ is attributed to high surface area of the Co–Cr–B catalyst powder as compared to Co–B catalyst.

However, the increment in active surface area of Co–Cr–B (χ_{Cr} = 4%) catalyst is about 2 times with respect to that of Co–B but the corresponding catalytic activity (maximum H_2 generation rate) increases by 4 times. This implies that Cr may possibly be involved in the catalytic hydrolysis reaction. To try to understand the role of Cr in the reaction it is important to consider the mechanisms of $NaBH_4$ hydrolysis involving the solid state catalyst. The H_2 production from the metal-catalyzed hydrolysis of $NaBH_4$ takes place, according to Ref. [11], by following kinetics steps: (1) BH_4^- ions are chemisorbed on the metal (Co) atoms; (2) H^- is transferred from BH_4^- to an unoccupied adjacent (Co) metal atom; (3) the hydrogen atom acquires an electron from the metal and leaves the site in hydridic form (H^-); (4) this H^- reacts with water molecule to produce H_2 and OH^-; and (5) OH^- reacts with boron in BH_3 to produce the $BH_3(OH)^-$ ion. Again, H^- is transferred from $BH_3(OH)^-$ ion to an unoccupied adjacent (Co) metal atom. The cycle of hydrogen absorption on metal sites continues till $BH_3(OH)^-$ forms $B(OH)_4^-$ and molecular hydrogen is released during each cycle.

According to the above hydrolysis reaction mechanism [11], the initial reaction occurs between BH_4^- ions and metal sites, which means that the reaction rate is proportional to the number of available metal sites for the absorption of BH_4^- ions in the solution. In the present scenario, the Co–Cr–B catalyst powder, having a surface area almost 2 times higher than that of Co–B, may provide an ideal condition for BH_4^- ions absorption for catalytic hydrolysis reaction. In addition, the electron-enriched metal active sites (Co^-) are able to facilitate the catalysis reaction by providing the electron required by hydrogen atom in the third step. However, during the last step the reaction between OH^- and BH_3^- ions is not favored by the catalyst, which may cause lower reaction rate. Thus, it is necessary to catalyze this reaction to enhance the overall reaction rate. In the present Co–Cr–B catalyst powder the surface Cr^{3+} species could act as Lewis acid sites, which are readily available for the absorption of Lewis base such as OH^- ions. During the hydrolysis reaction, the hydroxyl molecule in the solution can be absorbed on Cr^{3+} species via donating the lone electron from OH^- group. This bonding polarizes the hydroxyl group, which becomes favorable to the reaction with BH_3^- ions attached to the neighboring active Co sites. Similar kind of promoting effect by Cr metal was reported by Fang et al. [31] and Kukula et al. [43] using Ni–Cr–B and Co–Cr–B catalyst for hydrogenation of 2-ethylanthraquinone and nitriles, respectively. The authors showed that in both cases the Cr^{3+} species on the catalyst surface act as a Lewis acid sites and are readily able to increase absorption and reactivity of carbonyl [31] and nitrile [43] groups thus enhancing the overall catalytic activity as well as selectivity. Looking at these results, we may suggest that in our Cr-doped Co–B catalyst the presence of surface chromium oxide can improve absorption and reactivity of hydroxyl group thus explaining the observed higher activity with respect to that of the Co–B catalyst.

Additional experiments were performed to investigate the role of Cr during the hydrolysis of $NaBH_4$ in the presence of Cr-modified Co–B catalyst powder. In order to study the role of Cr^{3+} species in absorption of OH^- group for catalytic hydrolysis reaction, two types of hydride solution (0.025 M) were prepared, namely: (1) $NaBH_4$ solution stabilized with NaOH (0.025 M) (designated as solution A) and (2) $NaBH_4$ solution without NaOH (designated as solution B). In Fig. 6 we report hydrogen generation rate obtained

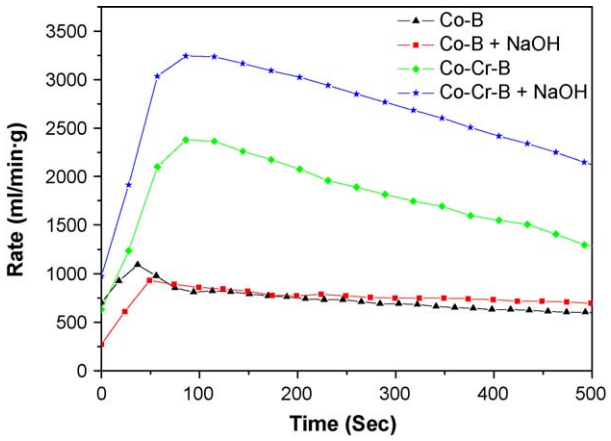

Fig. 6. Hydrogen generated rate as a function of reaction time obtained by hydrolysis of alkaline and non-alkaline $NaBH_4$ solution using Co–B, and Co–Cr–B (χ_{Cr} = 4%) catalyst powders.

by hydrolysis of solutions A and B using Co–Cr–B (χ_{Cr} = 4%) and Co–B catalyst powders. No significant change in H_2 generation rate was observed through hydrolysis of alkaline and non-alkaline $NaBH_4$ in the presence of Co–B catalyst powder. On the contrary, the H_2 generation rate obtained by hydrolysis of $NaBH_4$ in the presence of Co–Cr–B for solution A was much higher than that of solution B. This proves that during the hydrolysis reaction, in the presence of hydroxyl molecule in the solution, Cr^{3+} species are able to absorb the OH^- group and catalyze the reaction between OH^- and boron species (BH_3^-, $BH_2(OH)^-$, and $BH(OH)_2^-$). The R_{max} value measured with Co–Cr–B catalyst by hydrolysis of solutions A and B is 4 and 2.5 times higher than that obtained with the Co–B catalyst, respectively. Specifically, the increment in R_{max} observed with the Co–Cr–B catalyst during the hydrolysis of solution B, i.e., in the absence of OH^- group, is simply justified on the basis of the surface area of the catalyst, which is 2 times higher than that of Co–B. On the other hand, during the hydrolysis of alkaline solution A using the Co–Cr–B catalyst, both high surface area and capability of Cr^{3+} species to act as a Lewis absorption site for OH^- ions are involved in the major enhancement of R_{max} with respect to that observed with the Co–B catalyst.

3.4. Effect of solution temperature

Fig. 7 presents the H_2 generation yield as a function of time at different solution temperatures using alkaline $NaBH_4$ (0.025 M) solution and 15 mg of Co–Cr–B catalyst (χ_{Cr} = 4%) powder. The Arrhenius plot of the hydrogen production rate (inset of Fig. 7) gives an activation energy value of the catalytic hydrolysis process of about 37 ± 1 kJ mol^{-1}, which is lower than that obtained with Co–B powder (45 kJ mol^{-1}) [19], Raney Co (53.7 kJ mol^{-1}) [16] and Co–B nanoparticles (42.7 kJ mol^{-1}) [44]. This value is also lower than that found by Amendola (47 kJ mol^{-1}) [4] by using Ru catalyst. Kaufman and Sen [45], by using different bulk metal catalysts, obtained 75 kJ mol^{-1} for cobalt, 71 kJ mol^{-1} for nickel, and 63 kJ mol^{-1} for Raney nickel. The activation energy value obtained in the present case is comparable to that obtained with nanoparticle assembled Co–B thin film (30 kJ mol^{-1}) [29], Pd/C powder (28 kJ mol^{-1}) [46], Co supported on γ-Al_2O_3 (33 kJ mol^{-1}) [24], Ru nanoclusters (29 kJ mol^{-1}) [13] and Ru–C (37 kJ mol^{-1}) [47]. The favorable activation energy value obtained in the present work is attributed to both high surface area acquired by Co–Cr–B powder and promoting effect of Cr^{3+} species to enhance the catalytic hydrolysis reaction.

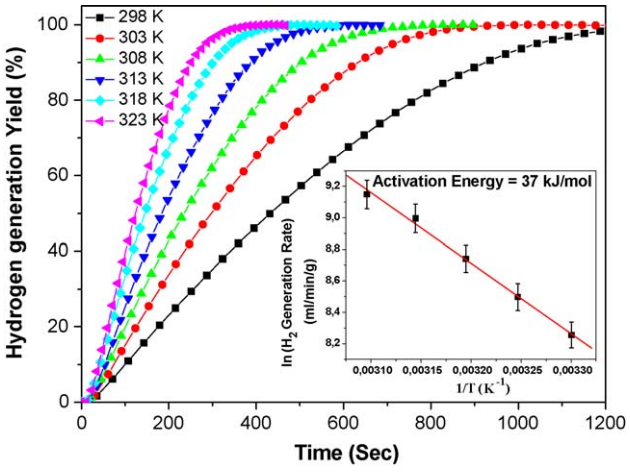

Fig. 7. Hydrogen generation yield as a function of reaction time by hydrolysis of alkaline $NaBH_4$ (0.025 M) solution with Co–Cr–B (χ_{Cr} = 4%) catalyst, measured at five different solution temperatures. Inset shows the Arrhenius plot of the H_2 generation rates.

3.5. Effect of $NaBH_4$ and NaOH

The effect of $NaBH_4$ concentration on the hydrogen generation rate was studied by performing a series of experiments using several concentrations of $NaBH_4$ while keeping catalyst and NaOH concentration constant. Fig. 8 presents the plot of hydrogen generated volume, as a function of time, obtained from hydrolysis of alkaline $NaBH_4$ solution by using four different $NaBH_4$ concentrations, namely: 0.05, 0.75, 0.10, and 0.15 M in the starting solution. The concentration of NaOH and Co–Cr–B catalyst (χ_{Cr} = 4%) was kept constant at 0.1 M and 15 mg, respectively, during the hydrolysis reaction. The figure clearly shows no significant changes in the hydrogen generation rate with the increase of the $NaBH_4$ concentration. Inset of Fig. 8 shows ln(R_{max}) vs ln(concentration of $NaBH_4$). The experimental points were fitted with a line having a slope of 0.09: the near-zero value of the slope indicates the zero order kinetics of the reaction with respect to the $NaBH_4$ concentration. The zero order of the reaction is explained on the basis that the initial hydride/catalyst molar ratio used for the measurement is high leading to BH_4^- induced dynamic saturation of the active sites on the catalyst [20]. Similar zero order kinetics was proposed by Amendola et al. [6] (Ru catalyst), Kojima et al. [48] (Pt–$LiCoO_2$), and Özkar et al. [13] (Ru nanoclusters) for reactions with high $NaBH_4$ concentration.

The hydrolysis reaction of $NaBH_4$ in water, without any catalyst, is suppressed by controlling the pH of the reaction solution; therefore, it is important to investigate the effect of NaOH concentration on the hydrolysis reaction. This was carried out by measuring the volume of the generated H_2 from hydrolysis of alkaline $NaBH_4$ by using five different NaOH concentrations, namely: 0.25, 0.50, 1, 1.85, and 2.5 M in the starting solution. The results are reported in Fig. 9. The concentration of $NaBH_4$ and Co–Cr–B catalyst (χ_{Cr} = 4%) was kept constant at 0.25 M and 15 mg, respectively, during the hydrolysis reaction. By increasing the NaOH content from 0.25 to 2.5 M, no change is observed in the hydrogen generation rate (R_{max}): this proves the zero order reaction with respect to NaOH concentration. This behavior can be explained in terms of $NaBH_4$ hydrolysis reaction mechanism, mentioned above, with the Co–Cr–B catalyst. The reaction between the boron species (BH_3^-, $BH_2(OH)^-$, and $BH(OH)_2^-$) and OH^- ions is catalyzed by absorption of OH^- ions on the Cr^{3+} surface species present in small amount. Thus a low initial concentration of OH^- ions is enough to dynamically cover these Cr^{3+} species and, as the

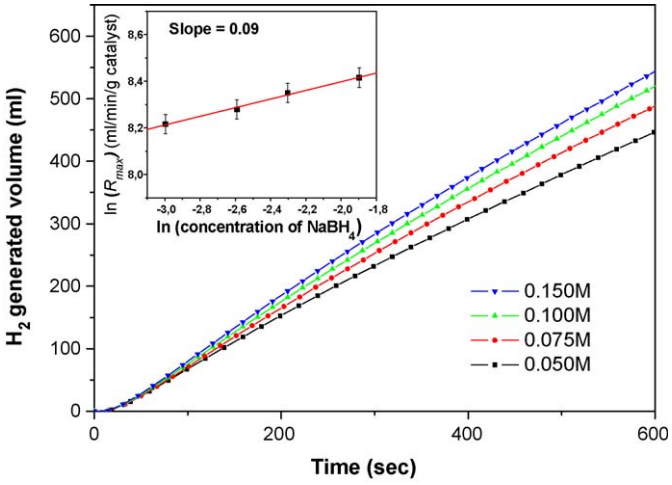

Fig. 8. Hydrogen generated volume as a function of reaction time with Co–Cr–B (χ_{Cr} = 4%) catalyst obtained by hydrolysis of alkaline $NaBH_4$ solution with four different concentrations of $NaBH_4$ ranging from 0.05 to 0.15 M. Inset shows the plot of ln(H_2 generation rate) vs ln(concentration of $NaBH_4$) to determine the reaction order with respect to $NaBH_4$.

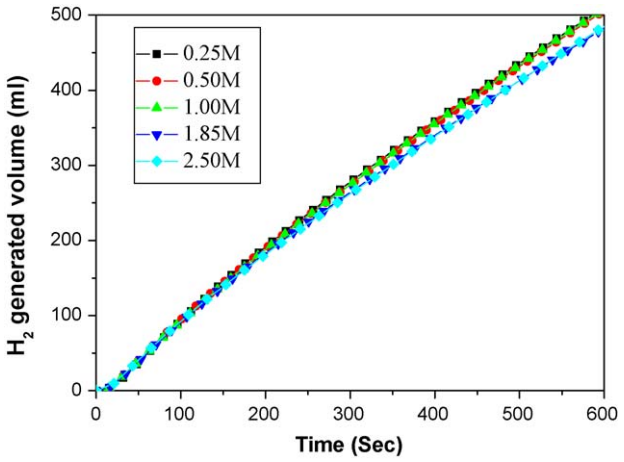

Fig. 9. Hydrogen generated volume as a function of reaction time with Co–Cr–B (χ_{Cr} = 4%) catalyst obtained by hydrolysis of alkaline $NaBH_4$ (0.25 M) solution with five different concentrations of NaOH ranging from 0.25 to 2.5 M. It is noticed that there is no relevant changes on generated hydrogen volume by changing the NaOH concentration.

reaction proceeds, the OH^- ions are provided by breaking of H_2O molecules. This explains the constant hydrogen generation rate at higher NaOH concentration.

4. Conclusions

We studied the catalytic activity of Cr-doped Co–B powder on hydrogen production by hydrolysis of $NaBH_4$. The rate of hydrogen production depends on the $\chi_{Cr} = Cr/(Cr + Co)$ parameter and the maximum value of the rate is observed when χ_{Cr} = 4% (the other parameters of the process being maintained constant). When χ_{Cr} is equal to 4% the catalytic activity is about 4 times higher than that of the pure Co–B catalyst. By characterization results, we found that this superior catalytic activity is related to the formation of chromium oxide, on the catalyst surface, which avoids agglomeration of the Co–B particles thus increasing the final active surface area of the Co–Cr–B powder catalyst. When the molar ratio χ_{Cr} is equal to 9% the BET surface area of the Co–Cr–B catalyst increases by one order of magnitude as compared to that of pure Co–B catalyst. Our experimental results also showed that Cr^{3+} species on the surface of the catalyst act as a Lewis absorption site for OH^- group and catalyze the reaction between OH^- and boron species thus increasing the overall reaction rate. The negative effect on catalytic activity at higher Cr-content, when χ_{Cr} exceeds 4%, is mainly attributed to surface covering of the active Co metal by Cr species. The promoting effect of Cr in Co–Cr–B catalyst results in a lower activation energy, for hydrogen production, which is 37 kJ mol^{-1} as compared to 45 kJ mol^{-1} of pure Co–B powder. The favorable activation energy is attributed to both high surface area acquired by Co–Cr–B powder and the possible role of Cr^{3+} species in the electron exchange mechanisms involved in the $NaBH_4$ hydrolysis with the Co–Cr–B catalyst.

Acknowledgements

We thank N. Bazzanella for SEM–EDS analysis, C. Armellini for XRD analysis, M. Filippi for XPS analysis, and S. Dirè for BET measurements. The research activity is financially supported by the Hydrogen-FISR Italian project.

References

[1] A.L. Dicks, J. Power Sources 61 (1996) 113.
[2] L. Schlapbach, A. Züttel, Nature 414 (2001) 353.
[3] L. Zhou, Renew. Sustain. Energy Rev. 9 (2005) 395.
[4] S.C. Amendola, S.L. Sharp-Goldman, M.S. Janjua, N.C. Spencer, M.T. Kelly, P.J. Petillo, M. Binder, Int. J. Hydrogen Energy 25 (2000) 969.
[5] R.B. Biniwale, S. Rayalu, S. Devotta, M. Ichikawa, Int. J. Hydrogen Energy 33 (2008) 360.
[6] S.C. Amendola, S.L. Sharp-Goldman, M.S. Janjua, M.T. Kelly, P.J. Petillo, M. Binder, J. Power Sources 85 (2000) 186.
[7] Z.P. Lin, N. Morigazaki, B.H. Liu, S. Suda, J. Alloys Compd. 349 (2003) 232.
[8] J. Lee, K.Y. Kong, C.R. Jung, E. Cho, S.P. Yoon, J. Han, T.-G. Lee, S.W. Nam, Catal. Today 120 (2007) 305.
[9] H.I. Schlesinger, H.C. Brown, A.B. Finholt, J.R. Gilbreath, H.R. Hockstra, E.K. Hydo, J. Am. Chem. Soc. 85 (1963) 215.
[10] Y. Bai, C. Wu, F. Wu, B. Yi, Mater. Lett. 60 (2006) 2236.
[11] G. Guella, C. Zanchetta, B. Patton, A. Miotello, J. Phys. Chem. B 110 (2006) 17024.
[12] P. Krishnan, T.H. Yang, W.Y. Lee, C.S. Kim, J. Power Sources 143 (2005) 17.
[13] S. Özkar, M. Zahmakiran, J. Alloys Compd. 404–406 (2005) 728.
[14] U.B. Demirci, F. Garin, Catal. Commun. 9 (2008) 1167.
[15] S. Suda, Y.M. Sun, B.H. Liu, Y. Zhou, S. Morimitsu, K. Arai, N. Tsukamoto, M. Uchida, Y. Candra, Z.P. Li, Appl. Phys. A: Mater. Sci. Process. 72 (2001) 209.
[16] B.H. Liu, Z.P. Li, S. Suda, J. Alloys Compd. 415 (2006) 288.
[17] S.U. Jeong, E.A. Cho, S.W. Nam, I.H. Oh, U.H. Jung, S.H. Kim, Int. J. Hydrogen Energy 32 (2007) 1749.
[18] N. Patel, G. Guella, A. Kale, A. Miotello, B. Patton, C. Zanchetta, L. Mirenghi, P. Rotolo, App. Catal. A: Gen. 323 (2007) 18.
[19] R. Fernandes, N. Patel, A. Miotello, M. Filippi, J. Mol. Catal. A: Chem. 298 (2009) 1.
[20] N. Patel, R. Fernandes, A. Miotello, J. Power Sources 188 (2009) 411.
[21] R. Fernandes, N. Patel, A. Miotello, Int. J. Hydrogen Energy 34 (2009) 2893.
[22] H. Li, H. Li, J. Zhang, W. Dai, M. Qiao, J. Catal. 246 (2007) 301.
[23] J. Zhao, H. Ma, J. Chen, Int. J. Hydrogen Energy 32 (2007) 4711.
[24] W. Ye, H. Zhang, D. Xu, L. Ma, B. Yi, J. Power Sources 164 (2007) 544.
[25] P. Krishnan, S. Advani, A.K. Prasad, Appl. Catal. B 86 (2009) 137.
[26] H.B. Dai, Y. Liang, P. Wang, H.M. Cheng, J. Power Sources 177 (2008) 17.
[27] D.-g. Tong, W. Chu, Y.-y. Luo, H. Chen, X.-y. Ji, J. Mol. Catal. A: Chem. 269 (2007) 149.
[28] H. Ma, W. Ji, J. Zhao, J. Liang, J. Chen, J. Alloys Compd. 474 (2009) 584.
[29] N. Patel, R. Fernandes, G. Guella, A. Kale, A. Miotello, B. Patton, C. Zanchetta, J. Phys. Chem. C 112 (2008) 6968.
[30] H. Li, J.F. Deng, J. Chem. Technol. Biotechnol. 76 (2001) 985.
[31] J. Fang, X. Chen, B. Liu, S. Yan, M. Qiao, H. Li, H. He, K. Fan, J. Catal. 229 (2005) 97.
[32] D.A. Lyttle, E.H. Jensen, W.A. Struck, Anal. Chem. 24 (1952) 1843.
[33] C. Zanchetta, B. Patton, G. Guella, A. Miotello, Meas. Sci. Technol. 18 (2007) N21.
[34] G.W. Pei, W.L. Zhong, S.B. Yue, Univ. Press Jinan (1989) 453.
[35] A. Baiker, Faraday Discuss. Chem. Soc. 87 (1989) 239.
[36] W.L. Dai, M.H. Qiao, J.F. Deng, Appl. Surf. Sci. 120 (1997) 119.
[37] A. Lebugle, U. Axelsson, R. Nyholm, N. Martensson, Phys. Scr. 23 (1981) 825.
[38] H. Li, H.X. Li, W.L. Dai, Z. Fang, J.F. Deng, Appl. Surf. Sci. 152 (1999) 25.
[39] H. Li, W. Wang, H. Li, J.F. Deng, J. Catal. 194 (2000) 211.
[40] H. Li, Y. Wu, H. Luo, M. Wang, Y. Xu, J. Catal. 214 (2003) 15.
[41] S. Yoshida, H. Yamashita, T. Funabiki, T. Yonezawa, J. Chem. Soc., Faraday Trans. 80 (1984) 1435.
[42] Handbook of X-ray Photoelectron Spectroscopy, Perkin Elmer Corporation, 1992
[43] P. Kukula, V. Gabova, K. Koprivova, P. Trtik, Catal. Today 121 (2007) 27.
[44] A. Garron, D. Swierczynski, S. Bennici, A. Auroux, Int. J. Hydrogen Energy 34 (2009) 1185.
[45] C.M. Kaufman, B. Sen, J. Chem. Soc., Dalton Trans. 2 (1985) 307.
[46] N. Patel, B. Patton, C. Zanchetta, R. Fernandes, G. Guella, A. Kale, A. Miotello, Int. J. Hydrogen Energy 33 (2008) 287.
[47] Y. Shang, R. Chen, Energy Fuels 20 (2006) 2149.
[48] Y. Kojima, K.I. Suzuki, Y. Kawai, J. Power Sources 155 (2006) 325.